

The VEGF receptor *flt-1* (VEGFR-1) is a positive modulator of vascular sprout formation and branching morphogenesis

Joseph B. Kearney, Nicholas C. Kappas, Catharina Ellerstrom, Frank W. DiPaola, and Victoria L. Bautch

Sprouting angiogenesis is critical to blood vessel formation, but the cellular and molecular controls of this process are poorly understood. We used time-lapse imaging of green fluorescent protein (GFP)-expressing vessels derived from stem cells to analyze dynamic aspects of vascular sprout formation and to determine how the vascular endothelial growth factor (VEGF) receptor *flt-1* affects sprouting. Surprisingly, loss of *flt-1* led to decreased sprout formation and migration, which resulted in reduced vascular

branching. This phenotype was also seen in vivo, as *flt-1*^{-/-} embryos had defective sprouting from the dorsal aorta. We previously showed that loss of *flt-1* increases the rate of endothelial cell division. However, the timing of division versus morphogenetic effects suggested that these phenotypes were not causally linked, and in fact mitoses were prevalent in the sprout field of both wild-type and *flt-1*^{-/-} mutant vessels. Rather, rescue of the branching defect by a soluble *flt-1* (sflt-1) transgene supports a model whereby *flt-1*

normally positively regulates sprout formation by production of sflt-1, a soluble form of the receptor that antagonizes VEGF signaling. Thus precise levels of bioactive VEGF-A and perhaps spatial localization of the VEGF signal are likely modulated by *flt-1* to ensure proper sprout formation during blood vessel formation. (Blood. 2004;103:4527-4535)

© 2004 by The American Society of Hematology

Introduction

The first step in the formation of most blood vessels is the production of an intricately branched vascular plexus.¹⁻³ This plexus is subsequently pruned and remodeled and in some cases coalesced to form larger vessels. The primary branched plexus forms by several processes, including the initial assembly of vascular precursor cells called vasculogenesis, and the subsequent migration of endothelial cells from the parent vessel called sprouting angiogenesis. The sprouts that form migrate until they reach another sprout or vessel, whereupon they most often form connections that are essential for elaborating and expanding the branched network. Although the formation of vascular sprouts has been described historically,⁴⁻⁶ surprisingly little is known of the cellular processes and molecular controls of sprout formation, and even less is known about how these processes are integrated with other ongoing cellular events such as cell division.

The vascular sprouts that form during embryonic development extend from primitive vessels. Individual endothelial cells send out filopodia, then migrate away from the parent vessel without breaking all contacts with surrounding cells, so that eventually multiple cells comprise the sprout. Cell numbers in the sprout are also increased by cell division behind the leading tip of the sprout.^{6,7}

Formation of a branched vascular plexus depends on the regulated expression of vascular endothelial growth factor-A

(VEGF-A) by nonendothelial cells. This signal modulates intracellular signaling pathways that regulate endothelial cell division, migration, and survival.⁸ This regulation is dose-dependent, as modest changes in the amount of available VEGF-A in either direction compromise vascular development, and loss of even one copy of the *Vegf-A* gene leads to vascular disruption and embryonic lethality.⁹⁻¹³ Availability also seems to be regulated by the production of different isoforms of VEGF-A via alternative splicing. These isoforms have differing affinities for matrix components, and disruption of individual isoforms affects vessel morphogenesis.¹⁴⁻¹⁶

VEGF-A signals through 2 receptor tyrosine kinases, flk-1 (VEGFR2) and *flt-1* (VEGFR1). VEGF/flk-1 interactions positively influence endothelial chemotaxis and proliferation, but the outcomes of VEGF/*flt-1* interactions are less clearcut.^{17,18} The *flt-1* gene encodes both a receptor tyrosine kinase (membrane *flt-1* [mflt-1]) and a secreted splice variant, sflt-1, which consists of the *flt-1* extracellular domain. The sflt-1 protein binds VEGF-A with high affinity and is a potent antagonist of VEGF/flk-1 signaling.^{19,20} Mouse mutants lacking *flt-1* die at embryonic day 9.5 with highly disorganized blood vessels and excess endothelial cells,²¹ yet a mouse with a modified *flt-1* gene that lacks most of the cytoplasmic domain is viable,²² suggesting that sflt-1 is sufficient for the developmental role of *flt-1*. We recently showed that *flt-1* negatively modulates endothelial cell division,²³ but the role of *flt-1* in

From the Program in Genetics and Molecular Biology, Dept of Biology, Carolina Cardiovascular Biology Center The University of North Carolina at Chapel Hill, Chapel Hill, NC.

Submitted July 9, 2003; accepted February 9, 2004. Prepublished online as *Blood* First Edition Paper, February 24, 2004; DOI 10.1182/blood-2003-07-2315.

Supported by National Institutes of Health (NIH) grants HL71993 and HL43174 (V.L.B.); a Department of Defense (DOD) predoctoral fellowship (J.B.K.); NIH Training Grant T32-HL69768 and an American Heart Association (AHA) predoctoral fellowship (N.C.K.); and postdoctoral support from The Swedish Foundation for International Cooperation in Research and Higher Education (STINT) and the Knut and Alice Wallenberg Foundation (C.E.).

J.B.K. and N.C.K. contributed equally to this work.

The online version of the article contains a data supplement.

An Inside *Blood* analysis of this article appears in the front of this issue.

Reprints: Victoria L. Bautch, Dept of Biology, CB# 3280, The University of North Carolina at Chapel Hill, Chapel Hill, NC 27599; e-mail: bautch@med.unc.edu.

The publication costs of this article were defrayed in part by page charge payment. Therefore, and solely to indicate this fact, this article is hereby marked "advertisement" in accordance with 18 U.S.C. section 1734.

© 2004 by The American Society of Hematology

endothelial cell migration remains unclear. In vitro studies, including analysis of chimeric VEGF receptors, failed to demonstrate a role for *flt-1* in endothelial migration.^{17,18,24-26} However, a study in which VEGF/*flt-1* binding was selectively blocked suggested that *flt-1* promotes VEGF-dependent actin reorganization and migration.²⁷

In the course of investigating the effects of a *flt-1* null mutation on blood vessel formation, we noticed aberrant morphogenesis of *flt-1*^{-/-} embryonic vessels.²³ Thus we reasoned that *flt-1* might modulate the VEGF-induced endothelial cell migration that occurs during embryonic sprouting angiogenesis. Our use of confocal time-lapse imaging afforded us the unique ability to analyze dynamic processes of mammalian vascular development. Vascular sprout formation was analyzed in wild-type and *flt-1*^{-/-} mutant embryonic stem (ES) cells induced to differentiate to form primitive vessels. To our surprise, *flt-1*^{-/-} blood vessels exhibited decreased sprout formation, and the *flt-1*^{-/-} mutant sprouts that formed had a reduced migration rate. Moreover, *flt-1*^{-/-} embryos showed defective sprouting of vessels from the dorsal aorta. This defect is likely not an immediate consequence of increased endothelial cell division in the mutant background, since the sprouting defect persisted after endothelial cell division rates returned to normal in *flt-1*^{-/-} mutant vessels. Rather, rescue of the mutant phenotype with an *sflt-1* transgene suggests a model whereby *sflt-1* protein interacts locally with VEGF-A. This interaction is predicted to establish or modify a gradient that regulates vascular sprouting and endothelial cell migration.

Materials and methods

Cell culture and in vitro differentiation

Wild-type (WT; +/+) and *flt-1*^{-/-} ES cells²¹ containing an enhanced green fluorescent protein (eGFP) or an *sflt-1* transgene under the transcriptional control of the platelet endothelial cell adhesion molecule (PECAM) promoter/intron enhancer element (P. Robson, D. Song, C.E., V.L.B., and H. S. Baldwin, manuscript in preparation) were maintained and differentiated in vitro as described previously.²⁸ Cultures were plated onto slide flasks (Nalge Nunc, Rochester, NY) at day 3 of differentiation and cultured at 37°C in 5% CO₂ until time-lapse imaging was performed.

DNA constructs and electroporation

The PECAM promoter/enhancer (gift of H. S. Baldwin; P. Robson, D. Song, C.E., V.L.B., and H. S. Baldwin, manuscript in preparation) was cloned into a modified eGFP vector (BD Clontech, Palo Alto, CA) for electroporation into WT ES cells and designated PECAM-eGFP. PGK-Hygro (gift of N. Maeda) was then inserted into the PECAM-eGFP vector for electroporation into *flt-1*^{-/-} ES cells and designated PECAM-eGFP-Hygro. The *sflt-1* cDNA was generated by reverse transcriptase-polymerase chain reaction (RT-PCR) amplification of a 500-base pair (bp) fragment of *sflt-1* (nucleotides [nt's] 1834-2544) from WT day-8 ES cell cultures, which was cloned via the TA method (Promega, Madison, WI) and verified by sequence analysis. A 2.1-kbp *Xba*I fragment from *mlt9* (mouse *flt-1* cDNA; gift of G. Breier²⁹) that encompassed nt's 1-2134 of full-length *flt-1* was cloned into the unique *Xba*I site at position 2134 of the *sflt-1* clone. The *sflt-1* cDNA was cloned into the PECAM-Hygro vector and designated PECAM-*sflt-1*.

Twenty micrograms of linearized PECAM-eGFP and PECAM-eGFP-Hygro DNAs were electroporated into 2×10^7 ES cells using a BioRad GenePulser II electroporator (250 V/300 μ F; BioRad, Hercules, CA). WT ES cell selection was in 200 μ g/mL G418 (Gibco, Carlsbad, CA), and selection of *flt-1*^{-/-} ES cells was in 200 μ g/mL hygromycin B (Roche Diagnostics, Indianapolis, IN). After 10 to 12 days, drug-resistant ES colonies were picked, expanded, and analyzed. We initially analyzed 3 WT transgenic lines (designated as WT; Tg pecam-egfp) and

4 *flt-1*^{-/-} transgenic lines (designated as *flt-1*^{-/-}; Tg pecam-egfp) and saw no differences except by genotype, so single WT and mutant lines were used. PECAM-eGFP and PECAM-*sflt-1* were linearized and electroporated into *flt-1*^{-/-} ES cells at a 1:3 molar ratio. After selection in hygromycin B, drug-resistant ES colonies that expressed eGFP were picked and analyzed.

Time-lapse imaging and quantitative analysis

Slide flasks containing day-6 to -8 in vitro-differentiated ES cultures were sealed, then placed on a heated stage on a Nikon TE300 inverted microscope (Melville, NY) with a Perkin Elmer spinning disk confocal head (Shelton, CT). Confocal images were acquired at 1-minute intervals using Metamorph software (version 6.0; Universal Imaging Corp, Downingtown, PA) and a Hamamatsu Orca CCD camera (McHenry, IL) with a $\times 20$ objective.³⁰ Quantitative image analysis was performed using Metamorph software. For sprout index measurements, total vessel perimeter was determined by outlining vessels and measuring total line length. Sprouts were defined as endothelial cell projections that included cytoplasm and were at least 10 μ m in length. For sprout velocity measurements, total sprout length was determined by measuring the distance from the tip of the sprout to the point at which the sprout joined the primary vessel wall. For cell division score measurements, average percentage of GFP-positive area was determined for each movie by thresholding and averaging 3 separate frames: the first, middle, and last frame. Significance was determined using the 2-tailed Student *t* test.

For fixed branch point analysis, cultures labeled with anti-PECAM antibody were photographed using a Nikon eclipse E800 upright microscope at $\times 10$ magnification. Vessel length was determined by tracing a vascular skeleton and measuring total line length using Metamorph software. Branch points were identified by visual scoring of each frame.

Antibody and β -galactosidase staining

Following time-lapse imaging, ES cell cultures were rinsed with phosphate-buffered saline (PBS) and fixed for 5 minutes in ice-cold methanol-acetone (50:50). Fixed cultures were reacted with rat antimouse PECAM at 1:1000 (MEC 13.3; BD Pharmingen, San Diego, CA) and donkey antirat immunoglobulin G (IgG; H+L) TRITC (tetramethylrhodamine-5 (and 6)-isothiocyanate) cross-absorbed at 1:100 (Jackson Immunoresearch, West Grove, PA) antibodies as described previously.^{12,28} All cultures were viewed and photographed with an Olympus IX-50 inverted microscope (Melville, NY) outfitted with epifluorescence. PECAM images were aligned with the last frame of each movie using Photoshop version 5.5 (Adobe Systems, San Jose, CA). Cocultures were fixed and processed for β -galactosidase reactivity as described.²³

Embryo manipulations

Flt-1^{+/-} mice were intercrossed, and embryos were dissected at 8.5 dpc (days after coitus) and fixed overnight in 4% paraformaldehyde (PFA) at 4°C. Yolk sacs were used for genotyping as described.²³ The next day embryos were dehydrated through a MeOH series then rehydrated and whole-mount stained for PECAM-1 as described.³¹ After staining, embryos were visualized and photographed on an Olympus SZH10 dissecting microscope.

Results

Dynamic image analysis of vascular sprout formation

To assay dynamic components of vascular morphogenesis, we generated stable ES cell subclones using a PECAM promoter/enhancer reporter in WT and *flt-1*^{-/-} genetic backgrounds (see "Materials and methods" for details). A subset of drug-resistant subclones expressed eGFP in the endothelial lineage upon differentiation. Because subclones of the same genotype were phenotypically similar, we chose a single WT line (P27; WT-eGFP) and a single *flt-1*^{-/-} line (GG5-15; *flt-1*^{-/-}-eGFP) for further analysis. To

confirm that expression of the reporter recapitulated expression of endogenous PECAM, we fixed day-8 WT-eGFP and *flt-1*^{-/-}-eGFP ES cell differentiation cultures after time-lapse image analysis and stained for PECAM (Figure 1). These images were overlaid with the last GFP image filmed (Figure 1Aiii,vi,ix). The congruence of the images showed that the eGFP reporters were expressed in the same cells that also expressed endogenous PECAM, and in all cases expression was associated with blood vessels. While the majority of PECAM-positive cells were endothelial cells lining the vessels, a small number of cells within the vessels also expressed PECAM, and these are likely to be the subset of hematopoietic cells that are PECAM positive. The apparent lack of eGFP expression in a subset of PECAM-positive cells results from the comparison of confocal (Figure 1Ai,iv,vii) with epifluorescence (Figure 1Aii,v,viii) images, since confocal images had a thinner focal plane. These data also confirm that the vascular phenotypes of the eGFP-expressing ES cell subclones recapitulate the parental vascular phenotypes.^{23,32} Specifically, a branched vascular plexus was seen in WT-eGFP cultures (Figure 1Ai-iii), while both sheets of endothelial cells (Figure 1Avii-ix) and some branched areas (Figure 1Aiv-vi) were seen in the *flt-1*^{-/-}-eGFP cultures. Finally, these results confirm that the conditions of time-lapse imaging do not adversely affect vascular development in the ES cell cultures.

We next asked whether a specific morphogenetic behavior, the formation of a vascular sprout, was recapitulated in ES cell

differentiation cultures (Figure 1B and Supplemental Movie S1, available at the *Blood* website; see the Supplemental Movies link at the top of the online article). Day-8 WT-eGFP ES differentiation cultures were imaged for 2 to 10 hours. The resulting images were examined for sprout formation, as defined by projections from the parent structure that were at least 10 μm in length and were GFP-positive. Numerous examples of sprout formation were noted, and one example is shown in Figure 1B. This sprout initiated, extended, and formed a connection with a sprout from another area within a 145-minute period. The eGFP reporter did not allow for precise location of cell boundaries, but the sprout length was approximately 20 μm at maximum, suggesting that it was composed of one or at most 2 endothelial cells. Most sprouts that formed in WT cultures either joined with another sprout or part of a vessel, or they remained in place as sprouts at the end of filming (Figure 2A; data not shown). Rarely, sprouts formed and retracted during the period of filming. These results show that ES cell differentiation is an appropriate model system for visualization and analysis of vascular morphogenetic processes in the mammal.

Sprout formation and function is compromised in the absence of flt-1

To determine how *flt-1* affects vascular morphogenesis at the cellular level, we next compared sprout formation between WT and *flt-1*^{-/-} vessels using dynamic image analysis (Figure 2A-B; Supplemental Movies S2-S3). Because *flt-1*^{-/-} ES cell cultures had areas of endothelial sheets, we were careful to score mutant sprout formation only in areas of *flt-1*^{-/-} ES cell cultures that contained a vascular plexus (Figure 1Aiv-vi; Figure 2Aiv-vi). To measure sprout formation, a sprout index that was normalized for time and vessel perimeter was calculated for multiple movies of each genotype. Since the lack of *flt-1* leads to increased rates of endothelial cell division via up-regulation of VEGF signaling,^{23,33} we hypothesized that morphogenetic parameters such as sprout formation would also be increased in the *flt-1*^{-/-} genetic background. To our surprise, *flt-1*^{-/-} vessels had a reduced sprout index relative to WT vessels. The sprout indices for day-6 and day-8 WT-eGFP time-lapse movies (Figure 2B, gray circles) had a wider distribution that ranged much higher than day-matched *flt-1*^{-/-}-eGFP movies (Figure 2B, black circles). Furthermore, *flt-1*^{-/-}-eGFP vessels showed a 2.5-fold decrease in average sprout formation index over day-matched WT controls. These results show that *flt-1*^{-/-} blood vessels sprout less often than WT blood vessels.

We next determined whether the absence of *flt-1* affects the rate of sprout migration. Analysis of time-lapse images was used to determine average sprout velocity (sprout vessel tip displacement/time) for *flt-1*^{-/-}-eGFP vascular sprouts and WT control sprouts (Figure 2C-D; Supplemental Movies S4-S5). Sprout vessel tips (Figure 2C, white arrowheads) were tracked over time using the base of the sprout at each time as the reference point. A plot of the average velocity for individual sprouts (Figure 2D) showed that *flt-1*^{-/-}-eGFP sprouts (black circles) displayed a lower range of velocities than WT-eGFP sprouts. Moreover, *flt-1*^{-/-}-eGFP sprouts had a mean average sprout velocity that was reduced by 36% compared with WT-eGFP sprouts. This result indicates that *flt-1* also modulates the speed with which sprouts migrate along a vector once they form.

We confirmed these results with a more traditional assay that is reflective of sprout formation: branch point analysis. Fixed samples of day-8 WT-eGFP and *flt-1*^{-/-}-eGFP differentiated ES cell cultures were labeled with PECAM to visualize vessels (Figure 3). The *flt-1*^{-/-}-eGFP and WT-eGFP vascular plexuses showed a range

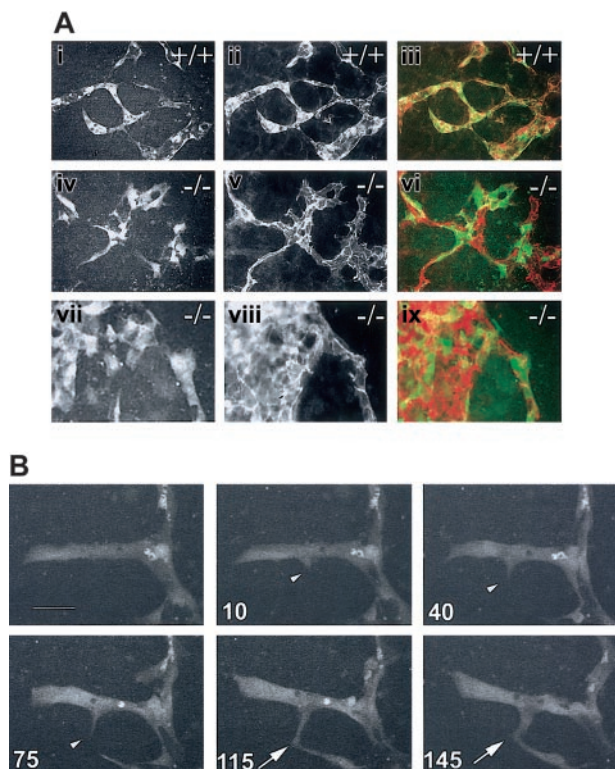


Figure 1. GFP expression allows for visualization of mammalian sprouting angiogenesis. Stable ES cell lines expressing PECAM-GFP were generated (see "Materials and methods") and subjected to time-lapse image analysis of vascular processes for 4.5 to 9.5 hours. (A) Day-8 WT-eGFP (+/+, i-iii) or *flt-1*^{-/-}-eGFP (-/-, iv-ix) ES differentiation cultures were imaged by time-lapse at 1-minute intervals for 4.5 to 9.5 hours, then fixed and reacted with an anti-PECAM antibody. The last frame captured (i,iv,vii) was overlaid (iii,vi,ix) with the PECAM-stained image (ii,v,viii). Original magnification $\times 20$. (B) Time-lapse frames of a day-8 WT-eGFP ES differentiation culture showing the formation of a vascular sprout and its fusion with another sprout. Time in minutes is at bottom left of each frame. The white arrowhead indicates sprout formation and extension; the white arrow, the fusion of the sprout tip with the second sprout. Scale bar in panel B is 20 μm (Supplemental Movie S1).

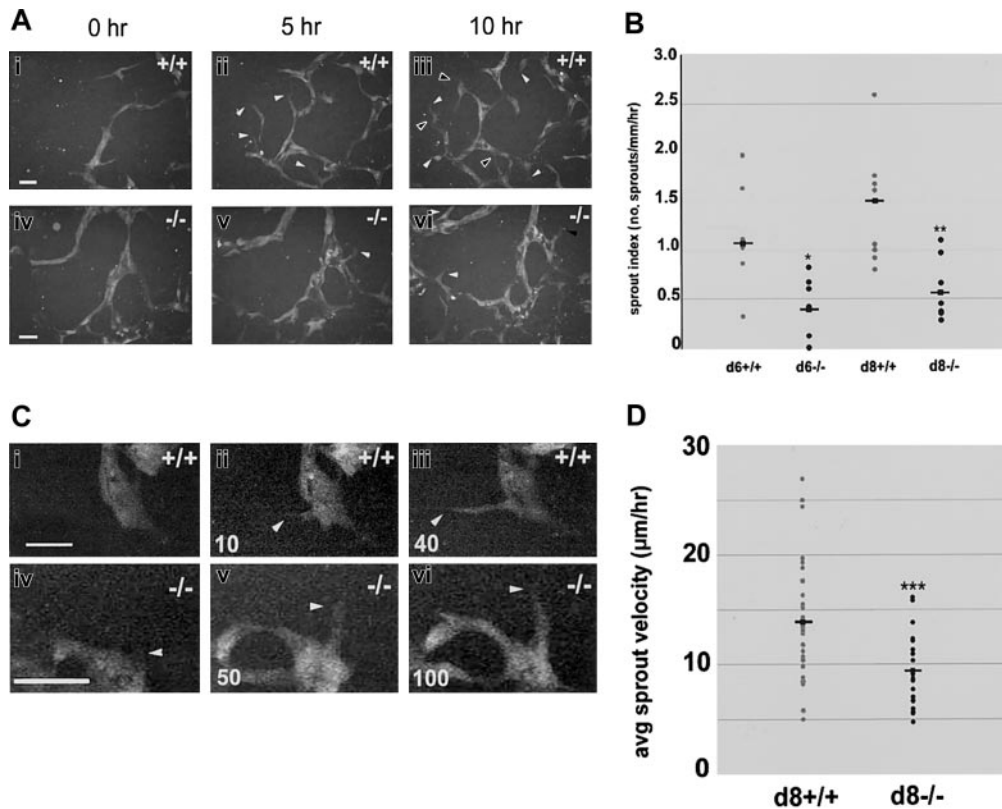


Figure 2. Sprout formation and migration are reduced in the absence of *flt-1*. Day-8 WT-eGFP (+/+; Ai-iii, Ci-iii) or *flt-1*^{-/-}-eGFP (-/-; Aiv-vi, Civ-vi) ES differentiation cultures were imaged by time-lapse at 1-minute intervals for the indicated times. (A) Over a 10-hour period, numerous new WT sprouts (i-iii) formed (white arrowheads) and remained or extended and/or fused at later times (black arrowheads), whereas very few *flt-1*^{-/-} sprouts (iv-vi) formed during the same time period. Scale bar is 20 µm (Supplemental Movies S2-S3). (B) Movie frames were analyzed to determine a sprout index (no. of sprouts/mm/h) for multiple movies on day 6 (d6) or day 8 (d8) of differentiation. Gray dots indicate WT-eGFP sprout indices; black dots, *flt-1*^{-/-}-eGFP sprout indices; and squares with lines, the average of each group. **P* < .03; ***P* < .01. (C) Over a 40-minute period, a WT sprout formed and extended between 30 and 40 µm, while over a 100-minute period a *flt-1*^{-/-} mutant sprout formed and extended only 20 µm. White arrowheads point to sprout tips, and time in minutes is at bottom left. Scale bar = 20 µm (Supplemental Movies S4-S5). (D) Movie frames were analyzed to determine average sprout velocity (µm/h) for multiple sprouts from different movies on day 8 (d8) of differentiation. Gray dots indicate WT-eGFP average sprout velocities; black dots, *flt-1*^{-/-}-eGFP average sprout velocities; and squares with lines, the average of each group. ****P* < .001.

of branch point densities (Figure 3A), but *flt-1*^{-/-}-eGFP ES cell cultures had less complex networks of blood vessels on average than WT controls (compare Figure 3Ai-iii with iv-vi). Quantitation showed that *flt-1*^{-/-}-eGFP ES cell cultures had a 30% to 40% decrease in branch point formation relative to WT (Figure 3B). Thus, the fixed branch point data are consistent with the time-lapse data, and they support a model whereby *flt-1* normally modulates vessel morphogenesis by positively regulating both the frequency of endothelial sprout formation and the rate of sprout migration.

To determine if the reduced sprout formation seen in the absence of *flt-1* was also seen in vivo, we examined the formation of intersomitic vessels that arise via sprouting angiogenesis from the dorsal aorta (Figure 4A). At 8.5 dpc, wild-type embryos consistently had several intersomitic vessels, and well-defined vascular sprouts were seen in register posterior to the vessels (Figure 4Ai-iii). In contrast, day-matched *flt-1*^{-/-} embryos had very few intersomitic sprouts, and those that formed were short and seldom connected to the vertebral vessel (Figure 4Aiv-vi). Thus the sprout defect documented in vascular development in ES differentiation cultures is also seen in mutant embryos lacking *flt-1*.

We reasoned that if sprout formation and migration were affected in the absence of *flt-1*, the endothelial cells at the tip of the sprout might have an abnormal morphology. Indeed, our examination of sprouts in *flt-1*^{-/-} embryos suggested that sprout tips tend to be blunted in the absence of *flt-1* (Figure 4Av inset,vi). To analyze this observation more carefully, we examined the morphologies of WT and *flt-1*^{-/-} mutant sprouts in ES cell differentiation cultures

(Figure 4B). WT sprout tips in general gradually tapered to a point, although rare WT sprouts were less tapered (Figure 4Bi-iv). In contrast, more of the *flt-1*^{-/-} mutant sprout tips were blunted (Figure 4Bv-viii), consistent with our findings that sprout migration along a vector is reduced.

Cell division defects are not immediately upstream of morphogenesis defects in *flt-1*^{-/-} mutant vessels

We previously showed that *flt-1*^{-/-} ES cultures display a 2- to 3-fold increase in endothelial cell division on day 6 of differentiation.²³ To determine if this difference was also observed with dynamic image analysis, we scored endothelial cell mitoses in *flt-1*^{-/-}-eGFP ES cell differentiation cultures and in WT controls (Figure 5; and Supplemental Movies S6-S7). Day-6 *flt-1*^{-/-}-eGFP cultures had increased numbers of mitotic endothelial cells compared with WT controls (compare Figure 5A and 5B). The number of endothelial cell divisions per hour was normalized for vascular area and used to produce a mitotic score that was averaged for multiple movies of both genotypes (Figure 5C). Day-6 *flt-1*^{-/-}-eGFP vessels had an average mitotic score that was increased over WT-eGFP vessels by more than 2-fold, consistent with our previous results.²³ However, the differences in mitotic score between WT and *flt-1*^{-/-} mutant vessels were resolved by day 8, a time point that was not assayed in our original study.

One explanation for the decreased frequency of sprout formation in the absence of *flt-1* is the possibility that the increased rate of

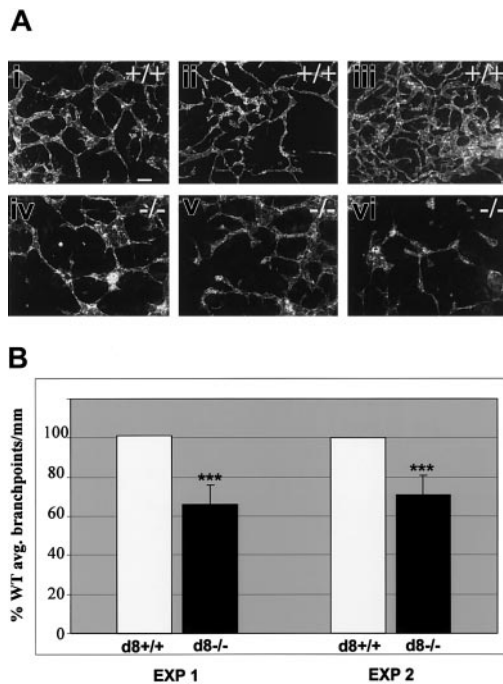


Figure 3. Branching morphogenesis is reduced in the absence of *flt-1*. Day-8 WT-eGFP (+/+; Ai-iii) or *flt-1*^{-/-}-eGFP (-/-; Aiv-vi) ES differentiation cultures were fixed and reacted with an anti-PECAM antibody. (A) Note that while each genotype had a range of branching complexities, on average less complexity was seen in the *flt-1*^{-/-}-eGFP cultures. Scale bar is 50 μ m. (B) The average number of branch points per millimeter of vessel length was determined using 10 fields of each genotype in 2 experiments and expressed as a percentage of wild-type branching. ****P* < .001.

cell division precludes sprout formation and migration. The fact that day-8 *flt-1*^{-/-}-eGFP cultures had the same mitotic score as day-matched WT controls, whereas the sprout index and sprout velocity were still significantly decreased at day 8 in the *flt-1*^{-/-} mutant vessels, suggests that this simple explanation is not valid. Time-lapse analysis provided the opportunity to observe the temporal and spatial positioning of endothelial cell divisions relative to sprout formation and maturation (Table 1). The sprout field was defined as the area of the primary vessel wall that would in the near future give rise to a sprout and the sprout itself. The rest of the structure was classified as primary vessel. Significant cell divisions occurred in the sprout field, and we even saw rare divisions in the distal-most tip cell of the sprout in both wild-type and *flt-1*^{-/-} mutant vessels (data not shown), indicating that cell division and sprout formation/migration are not mutually exclusive over time. Moreover, the distribution of mitoses between the primary vessel and the sprout field was similar between WT and *flt-1*^{-/-} mutant vessels on both days, indicating that the *flt-1* mutation does not change the distribution of endothelial mitoses.

Aberrant *flt-1*^{-/-} vascular morphogenesis is rescued in a non-cell-autonomous manner and with an *sflt-1* transgene

To begin to determine the mechanism whereby *flt-1* positively affects vascular morphogenesis, we asked whether *sflt-1*, the soluble antagonist of VEGF signaling, was generated coincident with vascular morphogenesis during ES cell differentiation. Day-8 wild-type and *flt-1*^{+/-} heterozygous ES differentiation cultures expressed *sflt-1* RNA and protein, and as predicted both RNA and protein were undetectable in day-matched *flt-1*^{-/-} ES differentiation cultures (data not shown). We reasoned that if *flt-1* positively regulates sprout formation via effects of the *sflt-1* protein, it might be possible to rescue the morphogenetic defect in *flt-1*^{-/-} vessels in

a non-cell-autonomous manner. To test this hypothesis, we cocultured wild-type and *flt-1*^{-/-} mutant embryoid bodies (EBs) in the same wells, by allowing EBs of both genotypes to attach on day 3 and continue differentiation to day 8 (Figure 6A). In contrast to *flt-1*^{-/-} vessels that consisted of large sheets with a few sprouts at the edges, *flt-1*^{-/-} vessels in wells with wild-type EBs (ratio of 3 WT to 1 mutant) showed areas of significant rescue and increased branching (compare Figure 6Ai to 6Aii). Thus the morphogenetic defect of *flt-1*^{-/-} vessels can be rescued in a non-cell-autonomous manner, suggesting that *sflt-1* and/or some other soluble component is critical to normal vascular morphogenesis.

To directly address the role of *sflt-1* in vascular morphogenesis, we reintroduced *sflt-1* into *flt-1*^{-/-} ES cells. A *PECAM-sflt-1* transgene was expressed in day-8 *flt-1*^{-/-}-*PECAM-sflt* cultures by RT-PCR (data not shown), and this was accompanied by a rescue of the mutant vascular phenotype (Figure 6B). A branch point analysis was performed, and the *flt-1*^{-/-}-*PECAM-sflt* cultures had rescued branching, with values that fell between WT and mutant cultures and that were significantly increased from *flt-1*^{-/-} cultures (Figure 6C).

Discussion

Our results show that *flt-1* modulates vascular sprout formation developmentally. To our surprise, this modulation is positive, and *flt-1* is required for proper sprout formation and migration. The data that support this conclusion are: (1) the rate of sprout formation and migration are both decreased in the absence of *flt-1*, (2) decreased

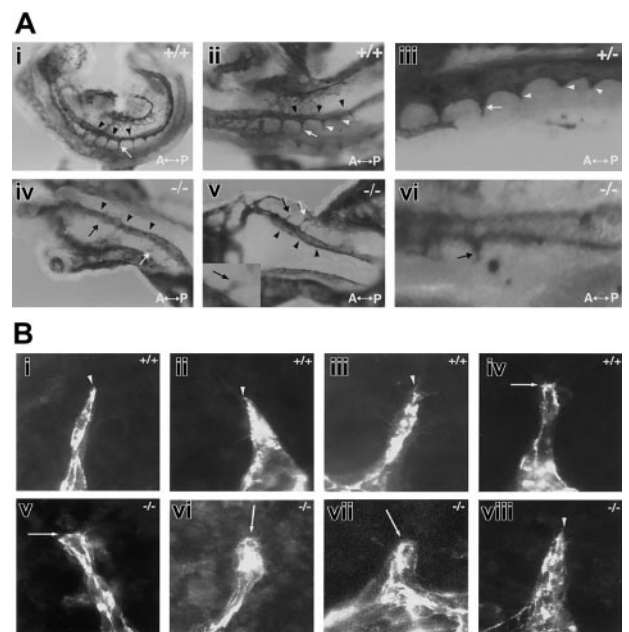


Figure 4. Sprouting from the dorsal aorta is reduced in the absence of *flt-1*. (A) The 8.5-dpc embryos that were WT (+/+; i-ii), *flt-1*^{+/-} (+/-; iii), or *flt-1*^{-/-} (-/-; iv-vi) were collected and whole-mount stained with an anti-PECAM antibody. (i-iii) In 3 different normal embryos, intersomitic vessels (white arrows) branch from the dorsal aorta (black arrowheads). A magnified view in panel iii shows several intersomitic sprouts (white arrowheads) in register posterior to the vessels. (iv-vi) Two different *flt-1*^{-/-} embryos show few branches from the dorsal aorta, and those that are seen are often stunted (black arrows). The inset in panels v and vi show stunted sprouts with blunted tips. A indicates anterior; and P, posterior. Original magnification \times 5. (B) Day-8 WT (i-iv) and *flt-1*^{-/-} (v-viii) ES differentiation cultures were fixed and stained with a PECAM antibody. Representative sprouts were photographed. Note that most WT sprouts are tapered at the distal end (white arrowheads), while most *flt-1*^{-/-} mutant sprouts are blunted (white arrows) at the distal end. Original magnification \times 60.

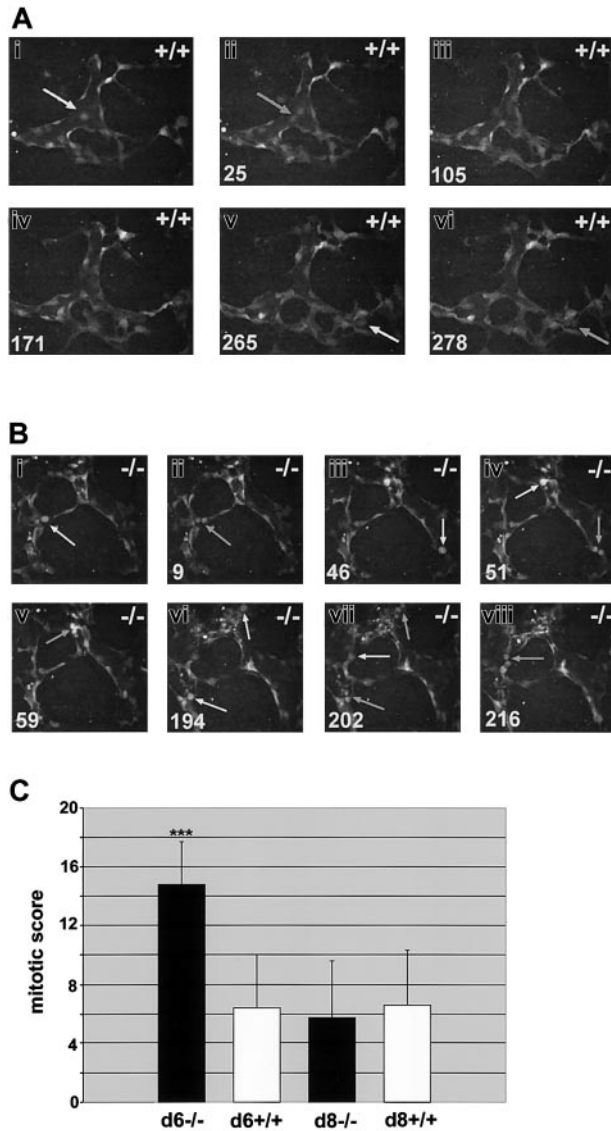


Figure 5. Endothelial cell divisions are increased in the absence of *flt-1*. Day-6 WT-eGFP (+/+; A) or *flt-1*^{-/-}-eGFP (-/-; B) ES differentiation cultures were imaged by time lapse at one-minute intervals for the indicated times. Day-8 cultures of both genotypes were also imaged for quantitation (C). (A-B) Endothelial cell predivision rounding up is denoted by white arrows, and cytokinesis is denoted by gray arrows. Time in minutes is at the bottom left. Note that over a similar time span there are more divisions scored in the *flt-1*^{-/-} mutant vessels (Supplemental Movies S6-S7). Original magnification × 20. (C) Time-lapse movies from day-6 WT-eGFP (n = 6), day-6 *flt-1*^{-/-}-eGFP (n = 8), day-8 WT-eGFP (n = 8), and day-8 *flt-1*^{-/-}-eGFP (n = 8) were analyzed for a mitotic score (no. of endothelial cell divisions/eGFP-positive area/h). ***P < .001.

Table 1. Distribution of endothelial cell divisions during sprout formation

Location in vessel	Day 6		Day 8	
	WT, % (23)	<i>flt-1</i> ^{-/-} , % (75)	WT, % (42)	<i>flt-1</i> ^{-/-} , % (38)
Primary vessel	78	75	90	91
Total sprout field	22	25	10	9
Proximal sprout area*	4	6	0	3
Distal sprout area	9	11	0	0
Nascent sprout area	9	8	10	6

The number in parentheses indicates the total number of cell divisions for each genotype. Numbers that are not bold are subdivisions of total sprout field. *Different compartments of the sprout field.

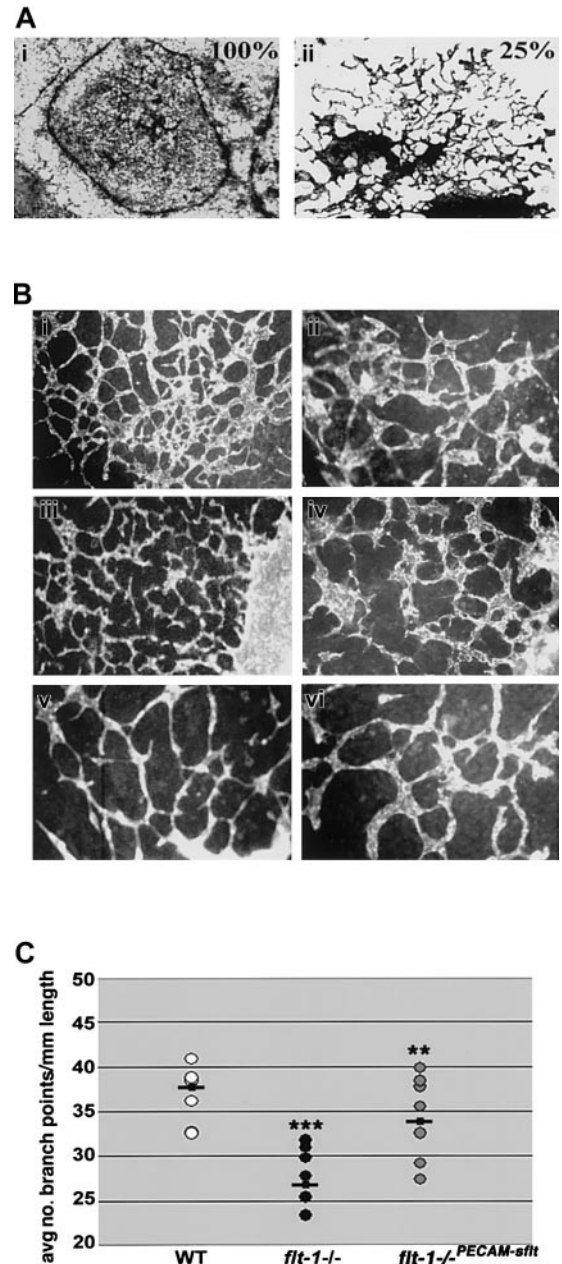


Figure 6. The *flt-1*^{-/-} phenotype is partially rescued non-cell-autonomously and by an *sflt-1* transgene. (A) Coculture analysis. Day-3 EBs were plated in wells so that (i) 100% were *flt-1*^{-/-} mutant EBs or (ii) 75% were WT and 25% were *flt-1*^{-/-} mutant EBs, and after attachment and incubation for a further 5 days, cultures were fixed and stained for β-galactosidase activity. Original magnification × 10. (B) Day-8 WT (Bi-ii), *flt-1*^{-/-} transfected with a PECAM-sflt transgene (Biii-iv), and *flt-1*^{-/-} (Bv-vi) ES differentiation cultures were fixed and reacted with an anti-PECAM antibody. Original magnifications × 10 (Bi,iii,v) and × 20 (Bii,iv,vi). Note that branching in *flt-1*^{-/-}-PECAM-sflt cultures more closely resembles WT than *flt-1*^{-/-} cultures. (C) The average number of branch points per mm of vessel length was determined using multiple fields of each genotype. **P < .01, *flt-1*^{-/-} versus *flt-1*^{-/-}-PECAM-sflt; ***P < .001, WT versus *flt-1*^{-/-}.

vascular branching accompanies loss of *flt-1* during ES cell differentiation and is rescued by an *sflt-1* transgene, and (3) decreased sprouting from the dorsal aorta results from loss of *flt-1* in vivo. Our data support a model whereby *flt-1* affects vascular morphogenesis via a soluble mediator that is likely to be *sflt-1*, suggesting that formation and/or modulation of a VEGF gradient may be important to the effect of *flt-1* on vascular sprout formation (Figure 7).

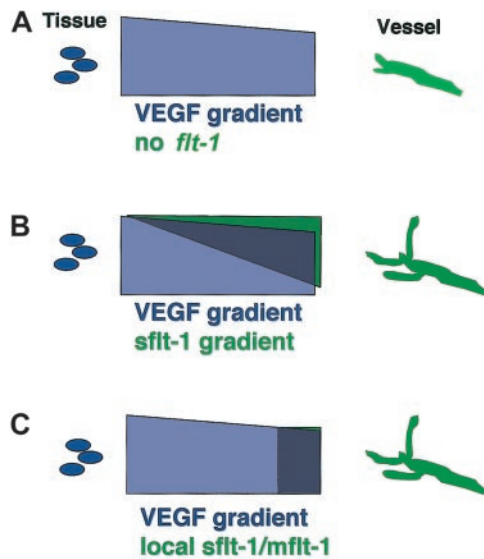


Figure 7. Models of *flt-1* modulation of VEGF signal-negative modulation results in net positive effect on sprout formation. We favor a model of *flt-1* action on sprout formation that results from *flt-1* binding VEGF-A and preventing binding to *flk-1* (see "Discussion" for details). This could occur in several ways. (A) VEGF-A may be deposited in a gradient between the producing tissue and the target vessel, and this unmodified gradient is not conducive to sprout formation in the absence of *flt-1*. (B) *sflt-1* may be secreted and form a counter-gradient that modifies and steepens the VEGF-A gradient, leading to increased sprout formation. (C) *mflt-1* and/or *sflt-1* may locally decrease the availability of VEGF-A, leading to increased sprout formation.

How does *flt-1* affect morphogenesis?

Since *flt-1*^{-/-} endothelial cells have a higher rate of division than do wild-type endothelial cells,²³ it was possible that the cell division defect was immediately upstream of the morphogenetic defect. That is to say, the endothelial cells possibly were too busy dividing to migrate. There is precedent for this model in that both normal and tumor vessels restrict cell divisions to sprout areas more proximal to the parent vessel,^{6,7,34} suggesting that actively migrating and sensing cells are prevented from dividing. Moreover, in tubulogenesis in the fly trachea, the tracheal precursor cell pool divides to produce all the tracheal cells, which then migrate and form the tracheal tubes in the absence of further cell division.³⁵

Our use of time-lapse image analysis allowed us to determine the relationship between cell division and cell migration with finer resolution than with end-point analyses, and it showed that endothelial cells in a migratory mode can also undergo cell division. The cells did not migrate during mitosis or for some time prior to mitosis, but once division was complete the daughter cells often migrated quite rapidly to resume sprout formation. We found that divisions were not excluded from the "sprout field" but in fact were in most cases enriched in the sprouts and their vicinity (N.C.K. and V.L.B., unpublished results), suggesting that sprout formation may stimulate cell division. We even on occasion saw the most distal cell of the sprout undergo mitosis in both WT and *flt-1*^{-/-} mutant vessels, although this event did not occur with high frequency. This finding differs from a recent study that found no tip cell division in retinal vessels.³⁴ However, retinal vessels track along a VEGF template provided by astrocytes, while in our model and in many developmental vascular beds the source of VEGF is likely to be more diffuse. Thus sprouts may have distinct phenotypes in response to different presentations of agonist. Finally, we saw no difference in the distribution of cell divisions to different areas of the vessel in the *flt-1*^{-/-} vessels compared with controls, indicating that *flt-1* does not regulate this parameter of cell division. It is formally possible that aberrant cell division in *flt-1*^{-/-}

mutant vessels somehow compromises sprout formation, since there are more endothelial cell divisions in the *flt-1* mutant background. However, the observation that the sprouting defects persist at day 8, when the rate of cell division in mutant vessels has returned to wild-type levels, strongly suggests that the effect of *flt-1* on sprout formation and extension is independent of cell division.

Flt-1 is a negative regulator of VEGF-A/*flk-1* signaling,^{19,33} and VEGF-A and *flk-1* are both expressed during ES cell differentiation and required for vessel formation.^{12,36} Thus the *flt-1*^{-/-} mutant vessels were expected to have increased sprout formation and migration. Instead, *flt-1*^{-/-} mutant sprouts formed less frequently and had slower migration rates. There are several models that are consistent with this phenotype. Perhaps VEGF signaling through the *flt-1* receptor (*mflt-1*) positively modulates endothelial cell migration developmentally, and the absence of this receptor in *flt-1* mutants blocks this positive migratory pathway. VEGF/*flt-1* signaling induces actin reorganization in cultured endothelial cells,²⁷ the *flt-1* kinase domain interacts with proteins involved in cell migration,³⁷ and a VEGFR1-blocking antibody decreases capillary connections in vitro.³⁸ However, a mouse model that lacks the *flt-1* kinase domain shows normal vascular development, and stimulation of retinal vessels with placental growth factor (PIGF), which binds *flt-1* but not *flk-1*, did not affect filopodia formation.^{22,34} These findings suggest that signaling through the *flt-1* receptor is not required for proper sprout formation developmentally.

Another possible model to explain reduced sprouting in the absence of *flt-1* is that *mflt-1* and/or *sflt-1* negatively modulate local interactions between VEGF-A and *flk-1* that are important for migration (Figure 7). *Flk-1* mediates VEGF-dependent endothelial cell migration, and VEGF/*flk-1* signaling affects focal adhesion kinase (FAK) and Src, molecules involved in focal adhesion signaling and turnover.^{24,39-41} VEGF/*flk-1* signaling also up-regulates the activity of the small guanine 5'-triphosphatase (GTPase) Rho,^{42,43} whose levels and spatial distribution are critical to proper migration as well.^{44,45} Indeed, recent work shows that cell migration involves the proper balance of adhesion and retraction of a cell, and imbalance in either parameter can impede movement.^{46,47} Thus the increased *flk-1* signaling in *flt-1*^{-/-} endothelial cells may lead to deregulation of Rho and/or focal adhesion turnover and thereby inhibit endothelial cell migration and sprout formation.

A model of vascular sprout formation

Our data are most consistent with a model of vascular sprout formation in which *flt-1* normally negatively regulates the amount of VEGF-A that is available to interact with the *flk-1* receptor, and this regulation provides the proper balance for a net positive effect on sprout formation and migration. Moreover, we show that the *flt-1*^{-/-} morphogenetic defect can be rescued in a non-cell-autonomous manner, that *sflt-1* is expressed appropriately to effect this rescue, and that an *sflt-1* transgene expressed via the PECAM promoter/enhancer can significantly rescue the aberrant branching. Thus, although we cannot exclude a role for surface-localized *mflt-1* in regulating the availability of VEGF-A, it is likely that *sflt-1* is the primary molecular mediator of sprout formation from the *flt-1* locus (Figure 7).

In our model, *sflt-1* is produced by endothelial cells and secreted into the local milieu, where it can interact with local sources of VEGF-A. VEGF-A secretion from nonendothelial cells induces migration toward the source of the signal. It is possible that *sflt-1* forms a protein gradient emanating from endothelial cells that interacts with VEGF-A to set up an effective VEGF gradient, or it could steepen an existing gradient (Figure 7B). *sflt-1* binds heparin

via IgG domain 4,⁴⁸ so it may bind the matrix and thus form a gradient. Alternatively, sflt-1 could modulate a preexisting VEGF-A gradient without forming an independent gradient (Figure 7C). VEGF-A has 3 major isoforms that result from alternative splicing, and they have different biochemical properties. The VEGF₁₂₀ isoform is completely diffusible, while the VEGF₁₆₅ and VEGF₁₈₈ isoforms are localized to the outer surface and surrounding matrix of VEGF-A-producing cells, although a significant fraction of VEGF₁₆₅ diffuses from the cell.¹⁴ Thus these isoforms could produce a VEGF-A gradient by virtue of their differing affinities for matrix, and sflt-1 could impact this gradient. In this scenario, *flt-1*^{-/-} mutant endothelial cells are inhibited from forming sprouts by exposure to excess VEGF-A (Figure 7A). Clearly, *flt-1*^{-/-} mutant blood vessels do form sprouts, so while sflt-1 may modulate sprout formation and migration, it is not absolutely required for sprouting angiogenesis.

What is the evidence for this model? Spatially localized VEGF expression predicts branching morphogenesis in the embryonic lung.⁴⁹ Analysis of retinal vessels in mouse mutants expressing only a single VEGF isoform demonstrates defects in vessel size and number, suggesting that the local availability and diffusion of VEGF-A protein is critical for vascular patterning during angiogenesis.¹⁵ A further analysis of VEGF isoform-selective mice provides evidence that a VEGF-A gradient set up in the hindbrain is compromised in the absence of matrix-bound VEGF.¹⁶ Moreover, inappropriate amounts of VEGF-A negatively affect sprout formation. Exogenous VEGF-A₁₆₅ injected into quail embryos inhibits the formation and branching of intersomitic vessels from the dorsal aorta,⁵⁰ similar to the effects seen in the *flt-1*^{-/-} mutant embryos in our study. A recent study in the eye showed that increased levels of each VEGF isoform led to reduced filopodia length and reduced expansion of the retinal vascular plexus.³⁴ These results suggest that excess VEGF-A leads to a perturbed endothelial migratory response, perhaps by disruption of a VEGF-A gradient, and support a model whereby *flt-1* negatively modulates local availability of VEGF-A to positively affect sprout formation.

The use of soluble receptors to modulate the activity of soluble ligands is not exclusive to the VEGF-A pathway. Other growth

factors, such as fibroblast growth factor (FGF), morphogens such as Wingless/Wnt, and vascular modifiers such as the angiopoietins, have soluble receptors of high affinity that can negatively modulate their respective signaling pathways.⁵¹⁻⁵⁵ Indeed, the soluble receptor frizzled-related protein (Frzb) is thought to form gradients that modulate the availability of Wingless to target cells.⁵² Thus, this molecular mechanism of signal regulation is conserved in other signaling pathways.

Conclusions

We have identified a novel role for *flt-1* in vascular morphogenesis, as a positive regulator of sprout formation and migration. This role is independent of a negative modulatory effect on endothelial cell division. We propose a model in which *flt-1* positively affects sprout formation by negatively controlling the amount of VEGF-A signal that is sensed by endothelial cells, using sflt-1 as the primary mediator of the effect. We also suggest that gradient formation, either by VEGF-A or sflt-1 or both proteins, may be important in modulating sprout formation and migration. In any case, these results have implications for the development of disease therapies and for reconstruction of vessels. Clearly, the local availability of VEGF-A signal is critical to proper morphogenesis, and the regulation of this availability under normal conditions appears complex. Thus a better understanding of how this is accomplished will allow for better design of regimens for vessel reconstitution.

Acknowledgments

We thank Guo Hua Fong for the *flt-1*^{+/-} and *flt-1*^{-/-} ES cells and for the *flt-1*^{+/-} mice, Georg Breier for the mouse *flt-1* cDNA, Nobuyo Maeda for the PGK-Hygro construct, and Scott Baldwin for making available the PECAM promoter/enhancer prior to publication. We thank the Bautch Lab members and the Carolina Cardiovascular Development Group for fruitful discussions.

References

- Daniel TO, Abrahamson D. Endothelial signal integration in vascular assembly. *Annu Rev Physiol.* 2000;62:649-671.
- Risau W. Mechanisms of angiogenesis. *Nature.* 1997;386:671-674.
- Drake CJ, Hungerford JE, Little CD. Morphogenesis of the first blood vessels. In: Fleischmajer R, Timpl R, Werb Z, eds. *Morphogenesis: Cellular Interactions.* Vol. 857. Annals of the New York Academy of Science. New York: NY Academy of Science; 1998:155-180.
- Sabin FR. Origin and development of the primitive vessels of the chick and of the pig. *Contrib Embryol Carnegie Inst.* 1917;6:61-124.
- Sabin FR. Studies on the origin of the blood vessels and of red blood corpuscles as seen in the living blastoderm of chick during the second day of incubation. *Contrib Embryol Carnegie Inst.* 1920;9:215-262.
- Clark ER, Clark EL. Microscopic observations on the growth of blood capillaries in the living mammal. *Am J Anat.* 1939;64:251-299.
- Ausprunk DH, Folkman J. Migration and proliferation of endothelial cells in preformed and newly formed blood vessels during tumor angiogenesis. *Microvasc Res.* 1977;14:53-65.
- Matsumoto T, Claesson-Welsh L. VEGF receptor signal transduction. *Sci STKE.* 2001;2001:RE21.
- Miquero L, Langille BL, Nagy A. Embryonic development is disrupted by modest increases in vascular endothelial growth factor gene expression. *Development.* 2000;127:3941-3946.
- Ferrara N, Carver-Moore K, Chen H, et al. Heterozygous embryonic lethality induced by targeted inactivation of the VEGF gene. *Nature.* 1996;380:439-442.
- Carmeliet P, Ferreira V, Breier G, et al. Abnormal blood vessel development and lethality in embryos lacking a single VEGF allele. *Nature.* 1996;380:435-439.
- Bautch VL, Redick SD, Scalia A, Harmaty M, Carmeliet P, Rapoport R. Characterization of the vasculogenic block in the absence of vascular endothelial growth factor-A. *Blood.* 2000;95:1979-1987.
- Damert A, Miquero L, Gertsenstein M, Risau W, Nagy A. Insufficient VEGFA activity in yolk sac endoderm compromises haematopoietic and endothelial differentiation. *Development.* 2002;129:1881-1892.
- Park JE, Keller GA, Ferrara N. The vascular endothelial growth factor (VEGF) isoforms: differential deposition into the subepithelial extracellular matrix and bioactivity of extracellular matrix-bound VEGF. *Mol Biol Cell.* 1993;4:1317-1326.
- Stalmans I, Ng YS, Rohan R, et al. Arteriolar and venular patterning in retinas of mice selectively expressing VEGF isoforms. *J Clin Invest.* 2002;109:327-336.
- Ruhrberg C, Gerhardt H, Golding M, et al. Spatially restricted patterning cues provided by heparin-binding VEGF-A control blood vessel branching morphogenesis. *Genes Dev.* 2002;16:2684-2698.
- Bernatchez PN, Soker S, Sirois MG. Vascular endothelial growth factor effect on endothelial cell proliferation, migration, and platelet-activating factor synthesis is Flk-1-dependent. *J Biol Chem.* 1999;274:31047-31054.
- Waltenberger J, Claesson-Welsh L, Siegbahn A, Shibuya M, Heldin CH. Different signal transduction properties of KDR and Flt1, two receptors for vascular endothelial growth factor. *J Biol Chem.* 1994;269:26988-26995.
- Kendall RL, Thomas KA. Inhibition of vascular endothelial cell growth factor activity by an endogenously encoded soluble receptor. *Proc Natl Acad Sci U S A.* 1993;90:10705-10709.
- Kendall RL, Wang G, Thomas KA. Identification of a natural soluble form of the vascular endothelial growth factor receptor, FLT-1, and its heterodimerization with KDR. *Biochem Biophys Res Commun.* 1996;226:324-328.
- Fong GH, Rossant J, Gertsenstein M, Breitman ML. Role of the Flt-1 receptor tyrosine kinase in regulating the assembly of vascular endothelium. *Nature.* 1995;376:66-70.
- Hiratsuka S, Minowa O, Kuno J, Noda T, Shibuya

- M. Flt-1 lacking the tyrosine kinase domain is sufficient for normal development and angiogenesis in mice. *Proc Natl Acad Sci U S A*. 1998;95:9349-9354.
23. Kearney JB, Ambler CA, Monaco KA, Johnson N, Rapoport RG, Bautch VL. Vascular endothelial growth factor receptor Flt-1 negatively regulates developmental blood vessel formation by modulating endothelial cell division. *Blood*. 2002;99:2397-2407.
 24. Gille H, Kowalski J, Li B, et al. Analysis of biological effects and signaling properties of Flt-1 (VEGFR-1) and KDR (VEGFR-2): a reassessment using novel receptor-specific vascular endothelial growth factor mutants. *J Biol Chem*. 2001;276:3222-3230.
 25. Rahimi N, Dayanir V, Lashkari K. Receptor chimeras indicate that the vascular endothelial growth factor receptor-1 (VEGFR-1) modulates mitogenic activity of VEGFR-2 in endothelial cells. *J Biol Chem*. 2000;275:16986-16992.
 26. Zeng H, Dvorak HF, Mukhopadhyay D. Vascular permeability factor (VPF)/vascular endothelial growth factor (VEGF) receptor-1 down-modulates VPF/VEGF receptor-2-mediated endothelial cell proliferation, but not migration, through phosphatidylinositol 3-kinase-dependent pathways. *J Biol Chem*. 2001;276:26969-26979.
 27. Kanno S, Oda N, Abe M, et al. Roles of two VEGF receptors, Flt-1 and KDR, in the signal transduction of VEGF effects in human vascular endothelial cells. *Oncogene*. 2000;19:2138-2146.
 28. Bautch VL, Stanford WL, Rapoport R, Russell S, Byrum RS, Futch TA. Blood island formation in attached cultures of murine embryonic stem cells. *Dev Dyn*. 1996;205:1-12.
 29. Breier G, Clauss M, Risau W. Coordinate expression of vascular endothelial growth factor receptor-1 (flt-1) and its ligand suggests a paracrine regulation of murine vascular development. *Dev Dyn*. 1995;204:228-239.
 30. Kearney JB, Bautch VL. *In vitro* differentiation of mouse ES cells: hematopoietic and vascular development. In: Wassarman PM, Keller GM, eds. *Methods in Enzymology: Differentiation of Embryonic Stem Cells*. Vol. 365. San Diego, CA: Elsevier Academic Press; 2003:83-98.
 31. Redick SD, Bautch VL. Developmental platelet endothelial cell adhesion molecule expression suggests multiple roles for a vascular adhesion molecule. *Am J Pathol*. 1999;154:1137-1147.
 32. Fong GH, Zhang L, Bryce DM, Peng J. Increased hemangioblast commitment, not vascular disorganization, is the primary defect in flt-1 knock-out mice. *Development*. 1999;126:3015-3025.
 33. Roberts DM, Kearney JB, Johnson JH, Rosenberg MP, Kumar R, Bautch VL. The VEGF receptor flt-1 (VEGFR-1) modulates flk-1 (VEGFR-2) signaling during blood vessel formation. *Am J Pathol*. 2004;164:1531-1535.
 34. Gerhardt H, Golding M, Fruttiger M, et al. VEGF guides angiogenic sprouting utilizing endothelial tip cell filopodia. *J Cell Biol*. 2003;161:1163-1177.
 35. Metzger RJ, Krasnow MA. Genetic control of branching morphogenesis. *Science*. 1999;284:1635-1639.
 36. Shalaby F, Ho J, Stanford WL, et al. A requirement for Flk1 in primitive and definitive hematopoiesis and vasculogenesis. *Cell*. 1997;89:981-990.
 37. Ito N, Wernstedt C, Engstrom U, Claesson-Welsh L. Identification of vascular endothelial growth factor receptor-1 tyrosine phosphorylation sites and binding of SH2 domain-containing molecules. *J Biol Chem*. 1998;273:23410-23418.
 38. Bussolati B, Dunk C, Grohman M, Kontos CD, Mason J, Ahmed A. Vascular endothelial growth factor receptor-1 modulates vascular endothelial growth factor-mediated angiogenesis via nitric oxide. *Am J Pathol*. 2001;159:993-1008.
 39. Abedi H, Zachary I. Vascular endothelial growth factor stimulates tyrosine phosphorylation and recruitment to new focal adhesions of focal adhesion kinase and paxillin in endothelial cells. *J Biol Chem*. 1997;272:15442-15451.
 40. Abu-Ghazaleh R, Kabir J, Jia H, Lobo M, Zachary I. Src mediates stimulation by vascular endothelial growth factor of the phosphorylation of focal adhesion kinase at tyrosine 861, and migration and anti-apoptosis in endothelial cells. *Biochem J*. 2001;360:255-264.
 41. Rousseau S, Houle F, Kotanides H, et al. Vascular endothelial growth factor (VEGF)-driven actin-based motility is mediated by VEGFR2 and requires concerted activation of stress-activated protein kinase 2 (SAPK2/p38) and geldanamycin-sensitive phosphorylation of focal adhesion kinase. *J Biol Chem*. 2000;275:10661-10672.
 42. van Nieuw Amerongen GP, Koolwijk P, Versteilen A, van Hinsbergh VW. Involvement of RhoA/Rho kinase signaling in VEGF-induced endothelial cell migration and angiogenesis in vitro. *Arterioscler Thromb Vasc Biol*. 2003;23:211-217.
 43. Zeng H, Zhao D, Mukhopadhyay D. KDR stimulates endothelial cell migration through heterotrimeric G protein Gq/11-mediated activation of a small GTPase RhoA. *J Biol Chem*. 2002;277:46791-46798.
 44. Ren X-D, Kioussis WB, Sieg DJ, Otey CA, Schlaepfer DD, Schwartz MA. Focal adhesion kinase suppresses Rho activity to promote focal adhesion turnover. *J Cell Sci*. 2000;113:3673-3678.
 45. Worthylake RA, Lemoine S, Watson JM, Burridge K. RhoA is required for monocyte tail retraction during transendothelial migration. *J Cell Biol*. 2001;154:147-160.
 46. Ridley AJ. Rho family proteins: coordinating cell responses. *Trends Cell Biol*. 2001;11:471-477.
 47. Etienne-Manneville S, Hall A. Rho GTPases in cell biology. *Nature*. 2002;420:629-635.
 48. Park M, Lee S-T. The fourth immunoglobulin-like loop in the extracellular domain of FLT-1, a VEGF receptor, includes a major heparin-binding site. *Biochem Biophys Res Commun*. 1999;264:730-734.
 49. Healy AM, Morgenthau L, Zhu X, Farber HW, Cardoso WV. VEGF is deposited in the subepithelial matrix at the leading edge of branching airways and stimulates neovascularization of the murine embryonic lung. *Dev Dyn*. 2000;219:341-352.
 50. Drake CJ, Little CD. Exogenous vascular endothelial growth factor induces malformed and hyperperfused vessels during embryonic neovascularization. *Proc Natl Acad Sci U S A*. 1995;92:7657-7661.
 51. Hanneken A, Ying W, Ling N, Baird A. Identification of soluble forms of the fibroblast growth factor receptor in blood. *Proc Natl Acad Sci U S A*. 1994;91:9170-9174.
 52. Moon RT, Brown JD, Yang-Snyder JA, Miller JR. Structurally related receptors and antagonists compete for secreted Wnt ligands. *Cell*. 1997;88:725-728.
 53. Gurdon JB, Bourillot PY. Morphogen gradient interpretation. *Nature*. 2001;413:797-803.
 54. Guillonnet X, Regnier-Ricard F, Laplace O, et al. Fibroblast growth factor (FGF) soluble receptor 1 acts as a natural inhibitor of FGF2 neurotrophic activity during retinal degeneration. *Mol Biol Cell*. 1998;9:2785-2802.
 55. Ruesch P, Barleon B, Weindel K, et al. Identification of a soluble form of angiopoietin receptor TIE-2 released from endothelial cells and present in human blood. *Angiogenesis*. 2001;4:123-131.